The Journal of Veterinary Medical Science

FULL PAPER

Pathology

Histopathological and immunohistochemical analysis of the cerebral white matter after transient hypoglycemia in rat

Nagi TOMITA[1,2], Tomoki NAKAMURA[1], Yuji SUNDEN[1] and Takehito MORITA[1]*

[1]Laboratory of Veterinary Pathology, Tottori University, Tottori, Tottori 680-8553, Japan
[2]The United Graduate School of Veterinary Science, Yamaguchi University, Yamaguchi, Yamaguchi 753-8511, Japan

J. Vet. Med. Sci.
82(1): 68–76, 2020
doi: 10.1292/jvms.19-0502

Received: 10 September 2019
Accepted: 17 November 2019
Advanced Epub:
2 December 2019

ABSTRACT. Patients with hypoglycemic coma show abnormal signals in the white matter on magnetic resonance imaging. However, the precise pathological changes in the white matter caused by hypoglycemic coma remain unclear in humans and experimental animals. This study aimed to reveal the distribution and time course of histopathological and immunohistochemical changes occurring in the white matter during the early stages of hypoglycemic coma in rats. Insulin-induced hypoglycemic coma of 15–30-min duration was induced in rats, followed by recovery using a glucose solution. Rat brains were collected after 6 and 24 hr and after 3, 5, 7, and 14 days. The brains were submitted for histological and immunohistochemical analysis for neurofilament 200 kDa (NF), myelin basic protein, olig-2, Iba-1, and glial fibrillary acidic protein (GFAP). Vacuolation was observed in the fiber bundles of the globus pallidus on days 1–14. Most of the vacuoles were located in GFAP-positive astrocytic processes or the extracellular space and appeared to be edematous. Additionally, myelin pallor and a decrease in NF-positive signals were observed on day 14. Microgliosis and astrogliosis were also detected. Observations similar to the globus pallidus, except for edema, were noted in the internal capsule. In the corpus callosum, a mild decrease in NF-positive signals, microgliosis, and astrogliosis were observed. These results suggest that after transient hypoglycemic coma, edema and/or degeneration occurred in the white matter, especially in the globus pallidus, internal capsule, and corpus callosum in the early stages.

KEY WORDS: edema, gliosis, hypoglycemia, rat, white matter

Hypoglycemia is a common complication of poor blood glucose control in diabetic patients [11, 20]. Severe hypoglycemia causes gray matter damage that is characterized by neuronal necrosis in the Cornu Ammonis 1 (CA1) of the hippocampus, dentate gyrus, subiculum, cerebral cortex, caudate, and putamen in experimental animals and humans [1, 4, 6, 7, 28]. In contrast, few reports have demonstrated pathological changes in the white matter, in response to severe hypoglycemia. Furthermore, Wallerian degeneration of axons accompanying with neuronal cytolysis occurs in the rat dentate gyrus and CA1 of hippocampus after severe hypoglycemia [5, 7]. However, to our knowledge, no studies have demonstrated histopathological and immunohistochemical findings in the white matter, including, axon, myelin, and oligodendrocytes, following exposure to severe hypoglycemia in rat brain. Some reports of human cases of hypoglycemia showed histological observations in the white matter, but they were often reported in severe and chronic cases, where it is difficult to detect primary changes [4, 28].

Recent reports have also demonstrated that in patients with severe hypoglycemia, abnormal signals were observed by diffusion-weighted magnetic resonance imaging (DWI) in the white matter such as the internal capsule, splenium of corpus callosum, globus pallidus, and/or centrum semiovale. Further, the distribution of abnormal signals had association with the patients' short-term outcomes [15, 16, 23, 24].

Therefore, there is a need of defining the histological and immunohistochemical characteristics of the white matter that are produced in response to transient severe hypoglycemia, using animal models. We aimed to generate an animal model of transient severe hypoglycemia and reveal the distribution and time course of histological and immunohistochemical findings in the white matter, especially in the regions of internal capsule, globus pallidus, and corpus callosum.

*Correspondence to: Morita, T.: morita@tottori-u.ac.jp

MATERIALS AND METHODS

Animals' procurement and ethical approval

Six-week-old male Sprague-Dawley (SD) rats were purchased from Clea Japan, Inc. (Tokyo, Japan) and allowed free access to tap water and food pellets (Clea Japan, Inc.). All protocols in this study were approved by the Animal Research Committee and were performed in accordance with the guidelines for animal experiments of the Faculty of Agriculture, Tottori University.

Hypoglycemic treatment

Male SD rats (210–310 g) were fasted overnight before the experiments, with access to tap water only. To induce hypoglycemic coma, rats were intra-peritoneally injected with 3.5–5.0 U/kg body weight of regular insulin (Novolin R, Novonordisk, Tokyo, Japan). Blood samples were collected from the caudal vein, and blood glucose levels were measured using a glucometer (Antsense III, HORIBA, Kyoto, Japan) every 30 min until 6 hr post-insulin administration with one final sample taken 24 hr post-insulin administration. Body temperatures were measured every hour until 6 hr post-insulin administration on representative rats (weighing environment logger, A&D Co., Ltd., Tokyo, Japan). Rats were anesthetized with 2–5% isoflurane (Intervet, Tokyo, Japan) in an anesthesia apparatus (DS Pharma Co., Ltd., Osaka, Japan) during the blood sampling and body temperature measurement. The onset of hypoglycemic coma was defined by low blood glucose levels (<20 mg/d*l*), absence of reaction to external stimuli and loss of corneal reflection. The hypoglycemic coma was maintained for 15–30 min. Rats then received a rapid intra-peritoneal injection of 50% glucose (0.5–1.5 m*l*) followed by frequent injections of a 1:1 mixture of 50% glucose and Krebs-Henseleit buffer (0.1–0.5 m*l* per injection; total of 1–3.5 m*l*) for 4 hr to terminate the hypoglycemic coma. As a control, sham hypoglycemic rats were given intra-peritoneal injection of insulin (3.5 U/kg) and 50% glucose simultaneously, followed by frequent injections of a 1:1 mixture of 50% glucose and Krebs-Henseleit buffer to maintain euglycemia. After recovery, all rats were provided free access to tap water and food pellets and kept until they were killed. Clinical signs were monitored throughout the hypoglycemic treatment and recovery period until the rats were killed.

Histological procedure

The rats were killed after 6 and 24 hr, and on days 3, 5, 7, and 14 (n=2–7 per group). Animals were deeply anesthetized by intra-peritoneal injection of pentobarbital sodium (64.8 mg/kg; Kyoritsu Seiyaku, Tokyo, Japan) and inhalation of 2–4% isoflurane. Then, they were intra-aortically perfused with 100 m*l* saline to wash the blood vessels, followed by 300 m*l* of 10% neutral phosphate-buffered formalin. Soon after perfusion, the brains were removed and sectioned coronally into 2-mm thick slices; two of the sections (Bregma −1.8 mm and −3.8 mm) were prepared for histological and immunohistochemical analyses. The brain sections were fixed with 10% neutral phosphate-buffered formalin again, immersed in ethanol and xylene, and then embedded in paraffin. Four-μm-thick paraffin sections were cut from each tissue block for hematoxylin and eosin staining, Klüver-Barrera (KB) staining, Bodian's staining, and immunohistochemistry.

Immunohistochemical procedure

Immunohistochemical analysis was performed using primary antibodies for glial fibrillary acidic protein (GFAP), ionized calcium-binding adaptor molecule 1 (Iba-1), myelin basic protein (MBP), neurofilament 200 kDa (NF), and oligodendrocyte transcription factor (olig-2). After de-paraffinization, sections were transferred into citric acid buffer (pH 6.0) and boiled for 20 min at 98°C in a microwave processor (MI-77, Azuma, Tokyo, Japan) to retrieve the antigens. Endogenous peroxidase activity was blocked with 3% hydrogen peroxide for 15 min and then the sections were pre-incubated with 10% normal goat serum for 30 min at room temperature. Next, the sections were incubated with a mouse monoclonal anti-GFAP antibody (diluted 1:400, Dako Denmark, Glostrup, Denmark), a rabbit polyclonal anti-Iba-1 antibody (diluted 1:2,000, Wako, Osaka, Japan), a mouse monoclonal anti-MBP antibody (diluted 1:1,000, Merck, Darmstadt, Germany), a mouse monoclonal anti-neurofilament antibody (diluted 1:500, Millipore, Burlington, MA, USA), or a rabbit polyclonal anti-olig-2 antibody (diluted 1:500, Millipore) at 4°C overnight. The reaction was revealed using 3, 3′-diaminobenzidine tetra-hydrochloride as a chromogen (Agilent, Tokyo, Japan), and counterstaining was performed with hematoxylin.

Scoring of histopathological and immunohistochemical alterations

We used histopathological and immunohistochemical parameters listed in Table 1 to objectively assess the degree of neuronal necrosis and white matter degeneration. Assessment of neuronal necrosis was performed in the neocortex, hippocampal dentate gyrus, CA1 of hippocampus, and caudoputamen. The assessment of white matter degeneration was performed in the globus pallidus, internal capsule, and corpus callosum. Each brain region was scored from 0 to 3 for each parameter, with the higher score indicating the more significant pathological condition. Six parameters of white matter degeneration were evaluated and the total score was obtained for each white matter region in each animal. Furthermore, the average scores of all animals that were killed at a particular point of time were obtained for each brain region.

Statistical analysis

Pearson's correlation coefficient was used to investigate the correlation between the score of neuronal necrosis and total score of white matter degeneration (the neocortex, hippocampal dentate gyrus, CA1 of hippocampus, or caudoputamen vs. the globus pallidus, internal capsule or corpus callosum) at each time-point. The test of significance for correlation coefficients was performed using two-sample, two tailed Student's *t*-test. Critical *P*-values <0.05 were considered statistically significant.

Table 1. Protocol of histopathological and immunohistochemical scoring system

Parameters	Score	Degree of pathological findings
Neuronal necrosis	0	None
	1	Occasionally
	2	Often
	3	Mostly
Variously sized vacuoles in the white matter (Vacuolation)	0	None
	1	Occasionally
	2	Often
	3	Densely
Decrease of NF-positive signals	0	Undetectable. Densely arranged axons with distinct positive signals
	1	Mild. Decreased density of axons with weak positive signals
	2	Moderate. Scattered axons with weaker and indistinct positive signals
	3	Marked. Rare positive signlas
Decrease of MBP-positive signals	0	Undetectable. Homogenous positive signals in a fiber bundle
	1	Mild. Inhomogenous positive signals in a fiber bundle
	2	Moderate. Negative signals in most part of each fiber bundle
	3	Marked. Rare positive signals
Decrease of olig-2-positive signals	0	Undetectable
	1	Mild. Diffusely weak positive signals
	2	Moderate. Scattered positive signals
	3	Marked. Rare positive signals
Increase of Iba-1-positive microglia (Microgliosis)	0	Undetectable
	1	Mild increase with activated morphology
	2	Moderate increase with activated morphology and occasional microglial nodules
	3	Marked increase with activated morphology and many microglial nodules
Increase of GFAP-positive astrocytes (Astrogliosis)	0	Undetectable
	1	Mild increase with slightly thickened dendrites
	2	Moderate increase with thickened dendrites
	3	Marked increase with hypertrophic morphology

NF: neurofilament 200 kDa, MBP: myelin basic protein, olig-2: oligodendrocyte transcription factor, Iba-1: ionized calcium-binding adaptor molecule 1, GFAP: glial fibrillary acidic protein.

RESULTS

Clinical observation of animals

Rats exhibited symptoms of severe hypoglycemia when blood glucose levels dropped below 20 mg/d*l* and subsequently went into a coma. Typically, the onset of the coma occurred within 2.5 hr after administration of insulin injection. All rats quickly recovered consciousness after administration of glucose injection. Blood glucose levels gradually increased and reached the pre-insulin injection levels within 3 hr after administration of glucose injection. The rats showed no significant change in breathing rate and body temperature during hypoglycemia and recovery. There were no significant neurological symptoms throughout the survival period following hypoglycemic treatment.

Histopathology

In the globus pallidus, one case showed spheroid-like changes in the fiber bundles 14 days after hypoglycemic coma (Fig. 1A). Vacuolation of the fiber bundles was observed in the globus pallidus from days 1 to 14 after hypoglycemic coma via KB staining, while neuronal necrosis was rarely noted in the gray matter of the globus pallidus (Fig. 2). One case on day 3 showed myelin debris in the fiber bundles of the globus pallidus that suggested myelin disruption. Myelin pallor was observed in the globus pallidus 14 days after hypoglycemic coma (Fig. 3). No significant changes in Bodian's staining were detected in any of the brain regions assessed.

Neuronal necrosis was observed in the neocortex, hippocampal dentate gyrus, hippocampal CA1 region, and caudoputamen (Table 2). There was diffuse neuronal necrosis in the neocortical layers II and III as early as 6 hr, and up to 14 days after hypoglycemic coma. Neuronal necrosis was observed in the dentate gyrus 6 hr and persisted up to 14 days after hypoglycemic coma, with the most severe cases appearing from 24 hr to 5 days after hypoglycemic coma. The crest of the dentate gyrus was the most commonly affected region exhibiting dense neuronal necrosis. In CA1 of the hippocampus, neuronal necrosis appeared 3 days after hypoglycemic coma and persisted up to 14 days after hypoglycemic coma. The most severe neuronal necrosis in the CA1 area was observed 3–5 days after hypoglycemic coma. The caudoputamen exhibited neuronal necrosis as early as 6 hr and up to 14 days after hypoglycemic coma, especially in lateral areas adjacent to the external capsule. The most severe neuronal necrosis in the caudoputamen was observed 3–7 days after hypoglycemic coma.

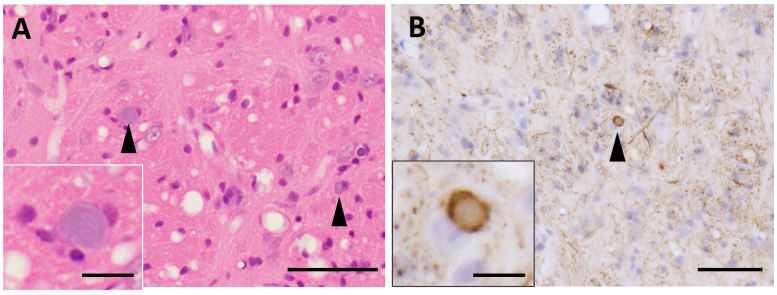

Fig. 1. Histopathological and immunohistochemical figures of the globus pallidus. Hematoxylin and eosin staining (A), immunohistochemistry for neurofilament 200 kDa (NF) (B). (A) 14 days after hypoglycemic coma. Spheroid-like structures were scattered in the fiber bundles (arrowheads). (A, Inset) High magnification of a spheroid-like structure. (B) 14 days after hypoglycemic coma. A NF-positive signal in the spheroid-like structure. (B, Inset) High magnification of a spheroid-like structure exhibiting NF-positive signal. Bar=50 μm, Insets: Bar=10 μm.

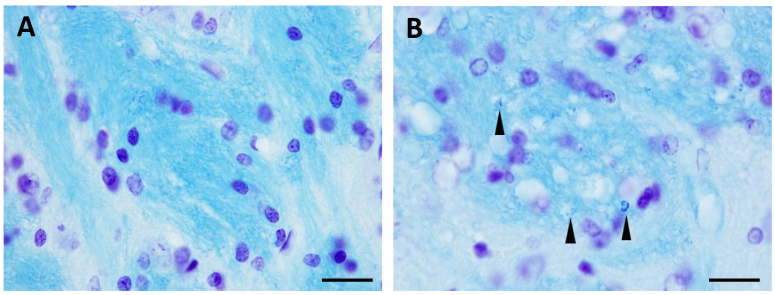

Fig. 2. Histopathological figures of the globus pallidus. Klüver-Barrera staining. (A) Sham-hypoglycemic coma (score 0). (B) 3 days after hypoglycemic coma. Vacuoles were observed in the fiber bundles (score 1). Myelin debris were scattered (arrowheads). Bar=20 μm.

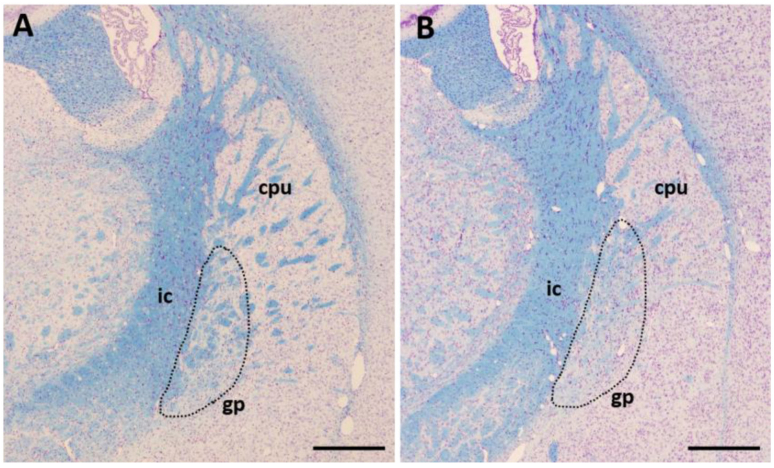

Fig. 3. Histopathological figures of the globus pallidus. Klüver-Barrera staining. (A) Sham-hypoglycemic coma. (B) 14 days after hypoglycemic coma. Myelin pallor in the grobus pallidus (broken line). ic: internal capsule, gp: globus pallidus, cpu: caudoputamen. Bar=500 μm.

Immunohistochemistry

NF-positive signals: NF-positive signals in the fiber bundles of the globus pallidus decreased 14 days after hypoglycemic coma. The number of NF-positive axons decreased and the remaining axons exhibited irregularly flattened shapes in cross sections (Fig. 4). The spheroid-like changes in the globus pallidus were associated with NF-positive signals in one case, 14 days after hypoglycemic coma (Fig. 1B). A decrease in NF-positive signals was also observed in the internal capsule 7 and 14 days after hypoglycemic coma. A mild decrease in NF-positive signals was noted in the corpus callosum on days 3, 5, 7, and 14.

MBP-positive signals: In the fiber bundles of the globus pallidus, a decrease of MBP-positive signals was not detected at 6 hr to 7 days; but was first observed 14 days post-hypoglycemic coma (Fig. 5). This pathology was detected irrespective of the presence of vacuolation in the fiber bundles of the globus pallidus. The vacuoles in the globus pallidus were occasionally delineated with MBP-positive signals (extracellular edema). The internal capsule exhibited a mild decrease of MBP-positive signals, 7 and 14 days

Table 2. Histopathological and immunohistochemical score and the number of animals exhibiting the finding in each time-point after hypoglycemic coma

		6 hr		24 hr		3 days		5 days		7 days		14 days	
		Score	n	Score	n	Score	n	Score	n	Score	n	Score	n
White matter													
Globus pallidus													
	Variously sized vacuoles in the white matter (Vacuolation)	0.0	0/2	1.0	1/2	0.6	3/5	0.5	1/4	0.8	2/4	0.3	1/7
	Decrease of NF-positive signals	0.0	0/1	0.0	0/1	0.0	0/5	0.0	0/3	0.0	0/2	0.7	3/6
	Decrease of MBP-positive signals	0.0	0/2	0.0	0/2	0.3	1/4	0.0	0/3	0.0	0/3	1.0	4/6
	Decrease of olig-2-positive signals	0.0	0/2	0.0	0/2	0.0	0/5	0.3	1/3	0.0	0/2	0.6	4/7
	Increase of Iba-1-positive microglia (Microgliosis)	1.0	2/2	0.5	1/2	0.8	3/5	0.5	1/4	1.7	2/3	1.7	7/7
	Increase of GFAP-positive astrocytes (Astrogliosis)	0.0	0/2	0.5	1/2	0.4	2/5	0.3	1/3	0.3	1/4	0.5	3/6
	Total score	1.0		2.0		2.1		1.6		2.8		4.8	
Internal capsule													
	Variously sized vacuoles in the white matter (Vacuolation)	0.0	0/2	0.0	0/2	0.0	0/5	0.0	0/4	0.0	0/4	0.0	0/7
	Decrease of NF-positive signals	0.0	0/1	0.0	0/1	0.0	0/4	0.0	0/3	0.3	1/3	0.7	3/6
	Decrease of MBP-positive signals	0.0	0/1	0.0	0/2	0.0	0/3	0.0	0/3	0.3	1/3	0.3	2/6
	Decrease of olig-2-positive signals	0.0	0/1	0.0	0/2	0.0	0/2	0.3	1/3	0.0	0/1	0.0	0/7
	Increase of Iba-1-positive microglia (Microgliosis)	0.5	1/2	0.5	1/2	0.5	2/4	0.3	1/3	0.3	1/4	1.0	5/6
	Increase of GFAP-positive astrocytes (Astrogliosis)	0.0	0/2	0.0	0/2	0.0	0/4	0.3	1/3	0.3	1/3	0.6	3/5
	Total score	0.5		0.5		0.5		0.9		1.2		2.6	
Corpus callosum													
	Variously sized vacuoles in the white matter (Vacuolation)	0.0	0/2	0.0	0/2	0.0	0/5	0.0	0/4	0.0	0/4	0.0	0/7
	Decrease of NF-positive signals	0.0	0/1	0.0	0/1	0.8	3/4	0.3	1/3	0.5	1/2	0.2	1/6
	Decrease of MBP-positive signals	0.0	0/2	0.0	0/2	0.0	0/5	0.0	0/4	0.0	0/4	0.0	0/7
	Decrease of olig-2-positive signals	0.0	0/1	0.0	0/2	0.0	0/5	0.3	0/3	0.0	0/2	0.0	0/7
	Increase of Iba-1-positive microglia (Microgliosis)	1.0	2/2	0.5	1/2	1.2	5/5	0.3	1/4	0.0	0/4	0.3	2/7
	Increase of GFAP-positive astrocytes (Astrogliosis)	0.0	0/2	0.0	0/2	0.2	1/5	0.0	0/4	0.0	0/4	0.1	1/7
	Total score	1.0		0.5		2.2		0.9		0.5		0.6	
Gray matter													
Cerebral neocortex	Neuronal necrosis	0.5	1/2	2.0	2/2	1.2	5/5	1.5	4/4	1.0	3/4	1.1	7/7
Dentate gyrus	Neuronal necrosis	1.0	2/2	1.5	2/2	1.2	4/5	1.0	2/4	0.5	2/4	0.7	4/7
CA1 of the hipocampus	Neuronal necrosis	0.0	0/2	0.0	0/2	0.8	3/5	1.3	4/4	0.5	2/4	0.3	2/7
Caudoputamen	Neuronal necrosis	1.0	2/2	1.0	2/2	1.6	5/5	1.0	3/4	1.3	3/4	0.7	4/7

Score: an average score of all animals included in the time point. n: the number of animals exhibiting the finding (score 1–3). NF: neurofilament 200 kDa, MBP: myelin basic protein, olig-2: oligodendrocyte transcription factor, Iba-1: ionized calcium-binding adaptor molecule 1, GFAP: glial fibrillary acidic protein.

after hypoglycemic coma.

Olig-2-positive signals: There was a decrease in the number of olig-2-positive oligodendrocytes in the globus pallidus 5 and 14 days after hypoglycemic coma (Fig. 6).

Iba-1-positive signals: There was an increase in the number of Iba-1-positive microglial cells in the globus pallidus, 6 hr to 14 days after hypoglycemic coma, with the greatest increase occurring between 3 and 14 days. At 6 hr post-hypoglycemic coma, the number of microglial cells increased in the globus pallidus with mildly thickened dendrites. On 1, 3, 5, 7, and 14 days post-hypoglycemic coma, microglial cells focally infiltrated into the fiber bundles of the globus pallidus (Fig. 7A and 7B). Some of the microglial cells exhibited an ameboid shape with short and thickened dendrites. While, some cases showed microgliosis without vacuolation, fiber bundle vacuolation was always accompanied by microglial infiltration. The number of Iba-1-positive cells increased in the internal capsule from 6 hr to 14 days after hypoglycemic coma and their highest infiltration was observed 14 days after hypoglycemic coma. Iba-1-positive microglial cells densely infiltrated from the external toward the ventral side of the internal capsule (Fig. 7C and 7D). In the corpus callosum, a mild increase in the number of Iba-1-positive microglial cells was observed in most cases from 6 hr to 5 days after hypoglycemic coma and in two cases on 14 days. Microglial cells occasionally appeared

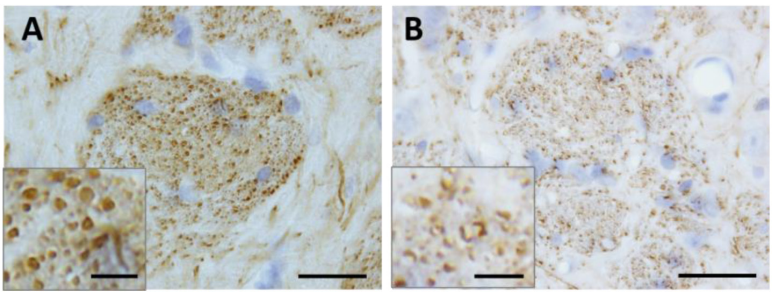

Fig. 4. Immunohistochemical figures of NF in the globus pallidus. (A) Sham-hypoglycemic coma. (A, Inset) High magnification of axons. Uniform cross-sections of NF-positive axons in the fiber bundles (score 0). (B) The globus pallidus 3 days after hypoglycemic coma. A decrease of NF-immunoreactivity in fiber bundles. (B, Inset) High magnification of axons. Cross sections of axons exhibited irregularly flattened shapes (score 1). Bar=20 μm, Insets: Bar=5 μm.

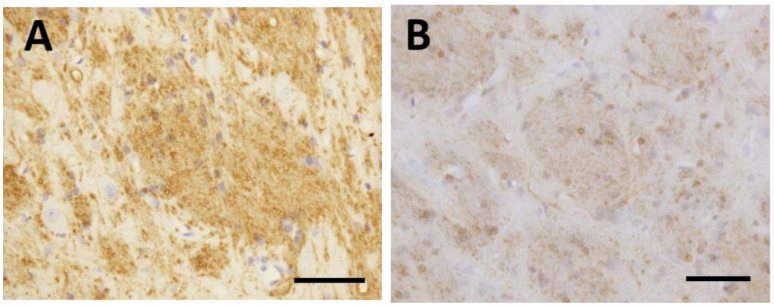

Fig. 5. Immunohistochemical figures of myelin basic protein in the globus pallidus. (A) Sham-hypoglycemic coma. Positive signals were observed in the fiber bundles (score 0). (B) 14 days after hypoglycemic coma. A significant decrease of immunoreactivity in the fiber bundles (score 2). Bar=50 μm.

rod-shaped and were situated along the neuronal fibers in the corpus callosum (Fig. 7E and 7F).

GFAP-positive signals: In the globus pallidus, the number of GFAP-positive astrocytes was increased on 1 day and up to 14 days after hypoglycemic coma. In fiber bundles of the globus pallidus, GFAP-positive astrocytes often contained vacuoles in their processes (intracellular edema) (Fig. 8). In the ventral region of the internal capsule, a mild increase in the number of GFAP-positive astrocytes was observed, 5–14 days post-hypoglycemic coma. A moderate activation of astrocytes in the corpus callosum was noted in a few cases on 3 and 14 days after hypoglycemic coma, and the activated GFAP-positive astrocytes exhibited slightly elongated dendrites.

Correlation between scores of gray matter regions and those of white matter regions

There was no significant correlation between the score of neuronal necrosis and total score of white matter degeneration in any combinations at any time-points (The date is not shown). In addition, two cases exhibited decrease in the NF, MBP, and olig-2 related immuno-reactivity and myelin pallor in the globus pallidus on 14 days after hypoglycemic coma, while the neuronal necrosis was not detected in the hippocampal CA1 and caudoputamen.

DISCUSSION

In this study, we revealed degeneration of axons, myelin, and/or oligodendrocytes in the globus pallidus, internal capsule and corpus callosum after transient hypoglycemic coma. The Wallerian degeneration of axons with neuronal cytolysis occurs in the rat dentate gyrus and hippocampal CA1 after hypoglycemia [5, 7]. However, to our knowledge, no reports have demonstrated histopathological and immunohistochemical characteristics in the white matter, including axons, myelin, and oligodendrocytes, after experimental hypoglycemic coma in the rat cerebrum. Therefore, this is the first report to demonstrate precise histopathological and immunohistochemical changes in axons, myelin, and oligodendrocytes with reaction of microglia and astrocytes in response to experimental hypoglycemic coma.

We also observed neuronal necrosis in CA1 of the hippocampus, subiculum, dentate gyrus, layers II and III of neocortex as well as caudoputamen that preceded the white matter degeneration. Of the brain regions showing neuronal necrosis after hypoglycemic coma, the caudoputamen have efferent projections to the globus pallidus, and the cerebral cortex has efferent projections to the internal capsule and corpus callosum [13, 18, 21, 27, 31]. Therefore, it might be possible that the degeneration of axons and myelin in the globus pallidus, internal capsule, and corpus callosum occurred secondarily to neuronal necrosis in the caudoputamen or

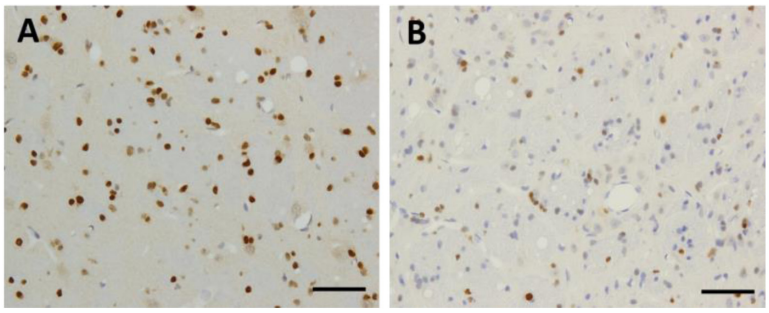

Fig. 6. Immunohistochemical figures of olig-2 in the globus pallidus. (A) Sham-hypoglycemic coma. Strong positive signals in oligodendrocytes (score 0). (B) 14 days after hypoglycemic coma. The number of olig-2 positive signals decreased and each signal was weak compared to that in sham-hypoglycemic control (score 1). Bar=50 μm.

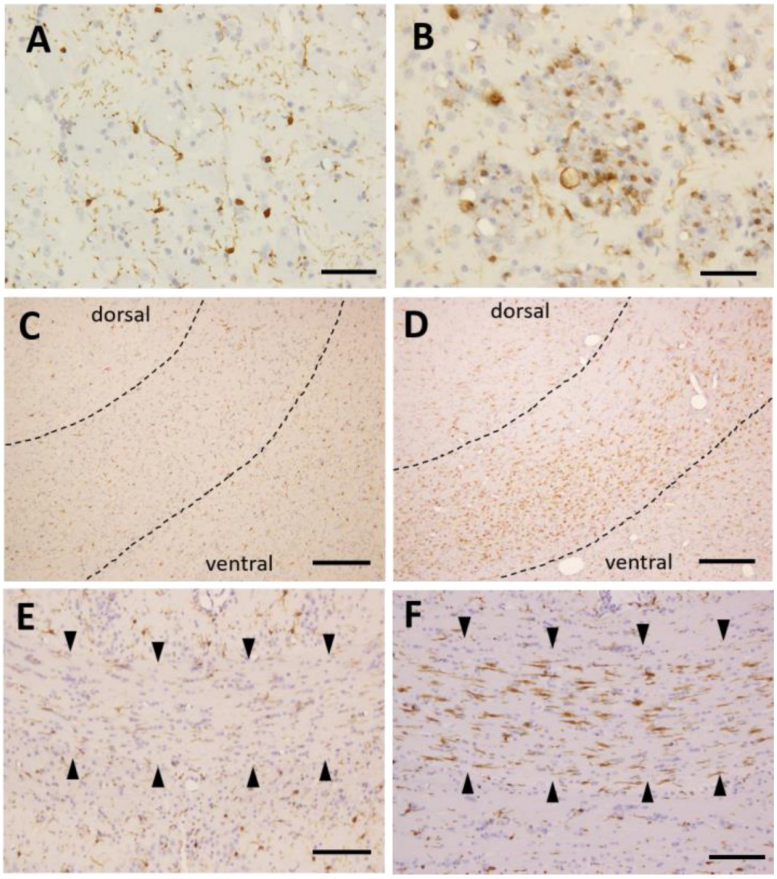

Fig. 7. Immunohistochemical figures of ionized calcium-binding adaptor molecule 1 (Iba-1) in the globus pallidus (A, B), the internal capsule (C, D) and the corpus callosum (E, F). (A) The globus pallidus of sham-hypoglycemic rat. Iba-1-positive microglial cells with thin dendrites were evenly distributed (score 0). (B) The globus pallidus 14 days after hypoglycemic coma. Iba-1-positive microglial cells focally infiltrated into the fiber bundles. Some microglial cells exhibited an ameboid shape with short and thickened dendrites (score 2). Bar=20 μm. (C) The internal capsule of sham-hypoglycemic coma (dashed lines) (score 0). (D) The internal capsule 14 days after hypoglycemic coma (dashed lines). Iba-1-positive microglial cells focally infiltrated into the ventral side of the internal capsule (score 2). Bar=100 μm. (E) The corpus callosum of sham-hypoglycemic rat (arrowheads) (score 0). (F) The corpus callosum 3 days after hypoglycemic coma (arrowheads). The number of Iba-1-positive microglial cells increased and they exhibited thickened rod-shaped dendrites (score 2). Bar=200 μm.

cerebral cortex. However, we could not find significant correlations between neuronal necrosis in the gray matter and pathological changes in the white matter. In addition, we found some cases in which white matter degeneration and microgliosis were present in the globus pallidus, without the occurrence of neuronal necrosis in the caudoputamen, 14 days after hypoglycemic coma. These results suggest that axonal degeneration can occur primarily after transient hypoglycemic coma independent of neuronal necrosis in the caudoputamen. Excitotoxicity is one of the most important factors in the pathogenesis of neuronal necrosis after

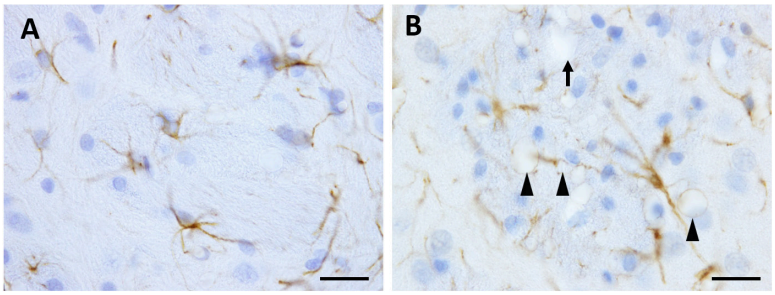

Fig. 8. Immunohistochemical figures of glial fibrillary acidic protein in the globus pallidus. (A) Sham-hypoglycemic coma (score 0). (B) 14 days after hypoglycemic coma. Some vacuoles were present in astrocytic processes (arrowheads). Others were present in extracellular spaces (an arrow) (score 1). Bar=20 μm.

severe hypoglycemia [3, 19]. The excitotoxic process is initiated by the release of excitatory amino acids, especially aspartate, in response to glucose deprivation that triggers the excess influx of Ca^{2+} into cells, and results in oxidative stress [19, 29, 30, 32]. Recent studies have demonstrated that excitotoxicity may also cause damage to the white matter [22, 26, 34]. In addition, a prior report demonstrated the microglial activation within 24 hr after excitotoxic brain damage in a neonatal mouse model [10]. In our study, early activation of microglia was observed in the white matter at 6 hr after hypoglycemic coma, preceding the degeneration of myelin and the decrease of NF- and olig-2-immunoreactivity. These findings suggest that excitotoxic processes could have contributed to the primary white matter damage.

We noted astrocytic-intracellular or extracellular edema in the globus pallidus 1–14 days post-hypoglycemic coma. Disruption of the blood brain barrier (BBB) is one of causes for edema after hypoglycemia [9, 12]. One previous report showed that disruption of the BBB caused by hypoglycemia occurred after 24 hr of recovery and contributed to edema formation [9]. In our study, edema in the globus pallidus appeared 1 day after hypoglycemic coma, which suggests that disruption of the BBB might contribute to the edema in the globus pallidus.

In contrast, edema was not detected in the internal capsule and the corpus callosum. Edema can also occur immediately after hypoglycemia before the recovery, when the BBB has not yet been disrupted [9, 12, 17]. Such edema in the early phase seems to result from an increase of intracellular Na^{+} because of the dysfunction of energy-dependent ion transporters [9].

Recent studies have reported regarding acute changes in patients with hypoglycemic coma, which were detected using diffusion-weighted MRI (DWI). The observations using DWI are valuable for detecting acute and primary brain damage in patients with severe hypoglycemia. DWI of hypoglycemic patients revealed hyperintensities and reduced apparent diffusion coefficients in the white matter, including the internal capsule and corpus callosum [2, 8, 15, 16, 24]. Abnormal DWI signals observed in hypoglycemia were considered to reflect intracellular edema [14, 24, 25, 33]. In human cases of hypoglycemia, abnormal DWI signals in the white matter were often observed during comatose hypoglycemia and disappeared immediately after recovery of consciousness by glucose injection [8, 23, 25]. These reports suggest that edema in the white matter rarely causes the BBB disruption and often disappears immediately after glucose injection in human cases of hypoglycemia. In our study, edema was only recognized in the globus pallidus, but not in the internal capsule and corpus callosum. It might be possible that the transient edema had in fact occurred; however, the BBB disruption did not occur, and the edema recovered because of glucose injection as seen in human studies [8, 23, 25].

In conclusion, we revealed that transient hypoglycemic coma causes white matter damage in the globus pallidus, internal capsule, and corpus callosum, and that the excitotoxic processes might have independently contributed to the primary white matter damage. We also defined the histopathological and immunohistochemical characteristics including extracellular and intracellular edema, axonal degeneration, myelin pallor, and activation of microglia and astrocytes. The prevention and/or treatment of the white matter damage may contribute to development of new strategies for the prevention and/or treatment of hypoglycemic brain damage. However, we need more investigation of the pathogenesis of the white matter damage in response to hypoglycemic coma, including the correlation between the white matter degeneration and edema.

REFERENCES

1. Agardh, C. D., Kalimo, H., Olsson, Y. and Siesjö, B. K. 1981. Hypoglycemic brain injury: metabolic and structural findings in rat cerebellar cortex during profound insulin-induced hypoglycemia and in the recovery period following glucose administration. *J. Cereb. Blood Flow Metab.* **1**: 71–84. [Medline] [CrossRef]
2. Aoki, T., Sato, T., Hasegawa, K., Ishizaki, R. and Saiki, M. 2004. Reversible hyperintensity lesion on diffusion-weighted MRI in hypoglycemic coma. *Neurology* **63**: 392–393. [Medline] [CrossRef]
3. Auer, R. N. 2004. Hypoglycemic brain damage. *Forensic Sci. Int.* **146**: 105–110. [Medline] [CrossRef]
4. Auer, R. N., Hugh, J., Cosgrove, E. and Curry, B. 1989. Neuropathologic findings in three cases of profound hypoglycemia. *Clin. Neuropathol.* **8**: 63–68. [Medline]
5. Auer, R., Kalimo, H., Olsson, Y. and Wieloch, T. 1985. The dentate gyrus in hypoglycemia: pathology implicating excitotoxin-mediated neuronal

necrosis. *Acta Neuropathol.* **67**: 279–288. [Medline] [CrossRef]
6. Auer, R. N., Olsson, Y. and Siesjö, B. K. 1984. Hypoglycemic brain injury in the rat. Correlation of density of brain damage with the EEG isoelectric time: a quantitative study. *Diabetes* **33**: 1090–1098. [Medline] [CrossRef]
7. Auer, R. N., Wieloch, T., Olsson, Y. and Siesjö, B. K. 1984. The distribution of hypoglycemic brain damage. *Acta Neuropathol.* **64**: 177–191. [Medline] [CrossRef]
8. Cordonnier, C., Oppenheim, C., Lamy, C., Meder, J. F. and Mas, J. L. 2005. Serial diffusion and perfusion-weighted MR in transient hypoglycemia. *Neurology* **65**: 175. [Medline] [CrossRef]
9. Deng, J., Zhao, F., Yu, X., Zhao, Y., Li, D., Shi, H. and Sun, Y. 2014. Expression of aquaporin 4 and breakdown of the blood-brain barrier after hypoglycemia-induced brain edema in rats. *PLoS One* **9**: e107022. [Medline] [CrossRef]
10. Dommergues, M. A., Plaisant, F., Verney, C. and Gressens, P. 2003. Early microglial activation following neonatal excitotoxic brain damage in mice: a potential target for neuroprotection. *Neuroscience* **121**: 619–628. [Medline] [CrossRef]
11. Donnelly, L. A., Morris, A. D., Frier, B. M., Ellis, J. D., Donnan, P. T., Durrant, R., Band, M. M., Reekie, G., Leese G. P. and DARTS/MEMO Collaboration. 2005. Frequency and predictors of hypoglycaemia in Type 1 and insulin-treated Type 2 diabetes: a population-based study. *Diabet. Med.* **22**: 749–755. [Medline] [CrossRef]
12. Gisselsson, L., Smith, M. L. and Siesjö, B. K. 1998. Influence of hypoglycemic coma on brain water and osmolality. *Exp. Brain Res.* **120**: 461–469. [Medline] [CrossRef]
13. Haring, J. H. and Wang, R. Y. 1986. The identification of some sources of afferent input to the rat nucleus basalis magnocellularis by retrograde transport of horseradish peroxidase. *Brain Res.* **366**: 152–158. [Medline] [CrossRef]
14. Hasegawa, Y., Formato, J. E., Latour, L. L., Gutierrez, J. A., Liu, K. F., Garcia, J. H., Sotak, C. H. and Fisher, M. 1996. Severe transient hypoglycemia causes reversible change in the apparent diffusion coefficient of water. *Stroke* **27**: 1648–1655, discussion 1655–1656. [Medline] [CrossRef]
15. Hegde, A. N., Mohan, S., Lath, N. and Lim, C. C. 2011. Differential diagnosis for bilateral abnormalities of the basal ganglia and thalamus. *Radiographics* **31**: 5–30. [Medline] [CrossRef]
16. Johkura, K., Nakae, Y., Kudo, Y., Yoshida, T. N. and Kuroiwa, Y. 2012. Early diffusion MR imaging findings and short-term outcome in comatose patients with hypoglycemia. *AJNR Am. J. Neuroradiol.* **33**: 904–909. [Medline] [CrossRef]
17. Kalimo, H., Auer, R. N. and Siesjö, B. K. 1985. The temporal evolution of hypoglycemic brain damage. III. Light and electron microscopic findings in the rat caudoputamen. *Acta Neuropathol.* **67**: 37–50. [Medline] [CrossRef]
18. Kincaid, A. E., Penney, J. B. Jr., Young, A. B. and Newman, S. W. 1991. The globus pallidus receives a projection from the parafascicular nucleus in the rat. *Brain Res.* **553**: 18–26. [Medline] [CrossRef]
19. Languren, G., Montiel, T., Julio-Amilpas, A. and Massieu, L. 2013. Neuronal damage and cognitive impairment associated with hypoglycemia: An integrated view. *Neurochem. Int.* **63**: 331–343. [Medline] [CrossRef]
20. Leese, G. P., Wang, J., Broomhall, J., Kelly, P., Marsden, A., Morrison, W., Frier, B. M., Morris A. D. and DARTS/MEMO Collaboration. 2003. Frequency of severe hypoglycemia requiring emergency treatment in type 1 and type 2 diabetes: a population-based study of health service resource use. *Diabetes Care* **26**: 1176–1180. [Medline] [CrossRef]
21. Leonard, C. M. 1969. The prefrontal cortex of the rat. I. Cortical projection of the mediodorsal nucleus. II. Efferent connections. *Brain Res.* **12**: 321–343. [Medline] [CrossRef]
22. Lima, R. R., Guimaraes-Silva, J., Oliveira, J. L., Costa, A. M., Souza-Rodrigues, R. D., Dos Santos, C. D., Picanço-Diniz, C. W. and Gomes-Leal, W. 2008. Diffuse axonal damage, myelin impairment, astrocytosis and inflammatory response following microinjections of NMDA into the rat striatum. *Inflammation* **31**: 24–35. [Medline] [CrossRef]
23. Lo, L., Tan, A. C., Umapathi, T. and Lim, C. C. 2006. Diffusion-weighted MR imaging in early diagnosis and prognosis of hypoglycemia. *AJNR Am. J. Neuroradiol.* **27**: 1222–1224. [Medline]
24. Ma, J. H., Kim, Y. J., Yoo, W. J., Ihn, Y. K., Kim, J. Y., Song, H. H. and Kim, B. S. 2009. MR imaging of hypoglycemic encephalopathy: lesion distribution and prognosis prediction by diffusion-weighted imaging. *Neuroradiology* **51**: 641–649. [Medline] [CrossRef]
25. Maekawa, S., Aibiki, M., Kikuchi, K., Kikuchi, S. and Umakoshi, K. 2006. Time related changes in reversible MRI findings after prolonged hypoglycemia. *Clin. Neurol. Neurosurg.* **108**: 511–513. [Medline] [CrossRef]
26. Matute, C., Alberdi, E., Domercq, M., Sánchez-Gómez, M. V., Pérez-Samartín, A., Rodríguez-Antigüedad, A. and Pérez-Cerdá, F. 2007. Excitotoxic damage to white matter. *J. Anat.* **210**: 693–702. [Medline] [CrossRef]
27. Molyneaux, B. J., Arlotta, P., Menezes, J. R. L. and Macklis, J. D. 2007. Neuronal subtype specification in the cerebral cortex. *Nat. Rev. Neurosci.* **8**: 427–437. [Medline] [CrossRef]
28. Mori, F., Nishie, M., Houzen, H., Yamaguchi, J. and Wakabayashi, K. 2006. Hypoglycemic encephalopathy with extensive lesions in the cerebral white matter. *Neuropathology* **26**: 147–152. [Medline] [CrossRef]
29. Norberg, K. and Siesiö, B. K. 1976. Oxidative metabolism of the cerebral cortex of the rat in severe insulin-induced hypoglycaemia. *J. Neurochem.* **26**: 345–352. [Medline] [CrossRef]
30. Patocková, J., Marhol, P., Tůmová, E., Kršiak, M., Rokyta, R., Stípek, S., Crkovská, J. and Anděl, M. 2003. Oxidative stress in the brain tissue of laboratory mice with acute post insulin hypoglycemia. *Physiol. Res.* **52**: 131–135. [Medline]
31. Preston, R. J., Bishop, G. A. and Kitai, S. T. 1980. Medium spiny neuron projection from the rat striatum: an intracellular horseradish peroxidase study. *Brain Res.* **183**: 253–263. [Medline] [CrossRef]
32. Sandberg, M., Butcher, S. P. and Hagberg, H. 1986. Extracellular overflow of neuroactive amino acids during severe insulin-induced hypoglycemia: in vivo dialysis of the rat hippocampus. *J. Neurochem.* **47**: 178–184. [Medline] [CrossRef]
33. Schaefer, P. W., Grant, P. E. and Gonzalez, R. G. 2000. Diffusion-weighted MR imaging of the brain. *Radiology* **217**: 331–345. [Medline] [CrossRef]
34. Yang, X., Hamner, M. A., Brown, A. M., Evans, R. D., Ye, Z. C., Chen, S. and Ransom, B. R. 2014. Novel hypoglycemic injury mechanism: N-methyl-D-aspartate receptor-mediated white matter damage. *Ann. Neurol.* **75**: 492–507. [Medline] [CrossRef]